

MULTILAYER WNbN/WNbC, WN/WC AND NbN/NbC COATINGS: VACUUM-ARC DEPOSITION STRATEGY AND MICROSTRUCTURE ASSESSMENT

**O.V. Maksakova^{a,b}, V.M. Beresnev^b, S.V. Lytovchenko^b, D.V. Horokh^b, B.O. Mazilin^b,
I.O. Afanasieva^{b,d}, M. Čaplovičová^c, Martin Sahul^a, V.A. Stolbovoy^d**

^a*Institute of Materials Science, Slovak University of Technology in Bratislava, 25, Jána Bottu Str., 917 24 Trnava, Slovakia*

^b*V.N. Karazin Kharkiv National University, 4, Svobody Sq., 61000 Kharkiv, Ukraine*

^c*Centre for Nanodiagnostics of Materials, Slovak University of Technology in Bratislava, Vazovova 5, 812 43 Bratislava, Slovakia*

^d*National Science Center «Kharkiv Institute of Physics and Technology», 1, Akademichna Str., Kharkiv, 61108, Ukraine*

*Corresponding Author e-mail: s.lytovchenko@karazin.ua

Received December 19, 2024; revised January 21, 2025; accepted February 14, 2025

Abstract. Reactive gases such as nitrogen, oxygen, and carbon-based gases (e.g., acetylene) are introduced into the generated plasma flow to create coatings with chemical compounds including nitrides, oxides, and carbides. By managing the rate of gas addition, the stoichiometric composition of the material, which influences its crystal structure and range of properties, can be controlled. In light of this, the vacuum-arc PVD technique was utilised to deposit carbide/nitride multilayer coatings based on W and Nb in a dynamically changing atmosphere of nitrogen and acetylene gases. The two-channel control device – “evaporator-injector” – was employed to control the functions of vacuum-arc evaporators and the gas introduction ports in the vacuum chamber of the installation. The material of the substrates for the deposition of coatings was corrosion-resistant high-temperature steel (grade 12X18H9T). The W (99.97 wt.%) and Nb (98.2 wt.%) cathodes were produced through mechanical boring of ingots made from the respective metals obtained via electron beam re-melting. The present work reports on the deposition strategy of vacuum-arc multilayer WNbN/WNbC, WN/WC, and NbN/NbC coatings with nanometre layer thicknesses and a preliminary assessment of their microstructure. The multilayer systems presented have yet to be studied and hold considerable scientific interest regarding synthesis and experimental investigation.

Keywords: Ceramic coatings; Tungsten nitride; Tungsten carbide; Niobium nitride; Niobium carbide; Vacuum-arc; Microstructure

PACS: 68.55.Jk, 68.65.Ac

INTRODUCTION

Because of the ease of use and excellent properties, physical vapour deposition (PVD) techniques are the most preferred method for applying hard protective coatings. PVD works by atomizing or vaporizing coating atoms from a target, transporting them through a vacuum or plasma, and then condensing them onto the substrate. PVD's widespread adoption in the industry can be attributed to its energy and cost-effectiveness, eco-friendliness, lower deposition temperatures (below 500 °C), higher deposition rates (up to 10 nm/s), increased flexibility in coating design, and outstanding coating quality [1-4]. Generally, PVD is categorized based on how the coating atoms are ejected from the target, which includes evaporative and sputtering processes. The growth mechanisms of hard coatings rely significantly on deposition conditions, plasma kinetics, and the physiochemical properties of the source elements.

Figure 1 depicts the recent PVD techniques used to create hard coatings alongside the key deposition parameters that affect the coatings' characteristics and functionality. Of these, magnetron sputtering methods are the most common for hard coating fabrication, mainly because they enable precise control over stoichiometry, microstructure, mechanical properties, and the creation of highly dense, defect-free, uniform coatings by adjusting various processing parameters. These include ion energy, ion flux, sputtering power, substrate bias, gas flow rate, partial pressure, and substrate temperature [5]. Various advanced sputtering techniques, such as balanced magnetron sputtering, radio frequency sputtering, reactive sputtering, and high-power impulse magnetron sputtering, are commonly employed in fabricating hard coatings. Additionally, laser deposition (LD) methods, along with their hybrid combinations with magnetron sputtering, have gained traction for extreme environmental applications in recent years [6,7].

Nevertheless, evaporative PVD methods remain predominant in industrial coating production, owing to their higher ionisation and deposition rates, more uniform coatings, and less stringent vacuum requirements [1,2]. The PVD process based on evaporation can employ various heat sources such as resistance, induction, electron beam, and arc sources, including arc discharge, filtered cathodic vacuum arc (FCVA), electron beam PVD, and thermal evaporation. The limitations of resistance, induction, and electron beam evaporative PVD systems render arc evaporative PVD systems more appealing compared to their industrial counterparts. For instance, resistive systems face electron beam systems encounter gun deterioration and substrate geometry restrictions [8], induction systems tend to be expensive [9,10], and melting point limitations [11]. Furthermore, arc evaporation PVD systems provide increased versatility, superior ionisation, adaptable target configurations, and a high deposition rate [1,8].

Cite as: O.V. Maksakova, V.M. Beresnev, S.V. Lytovchenko, D.V. Horokh, B.O. Mazilin, I.O. Afanasieva, M. Čaplovičová, M. Sahul, V.A. Stolbovoy, East Eur. J. Phys. 1, 396 (2025), <https://doi.org/10.26565/2312-4334-2025-1-49>

© O.V. Maksakova, V.M. Beresnev, S.V. Lytovchenko, D.V. Horokh, B.O. Mazilin, I.O. Afanasieva, M. Čaplovičová, M. Sahul, V.A. Stolbovoy, 2025; CC BY 4.0 license

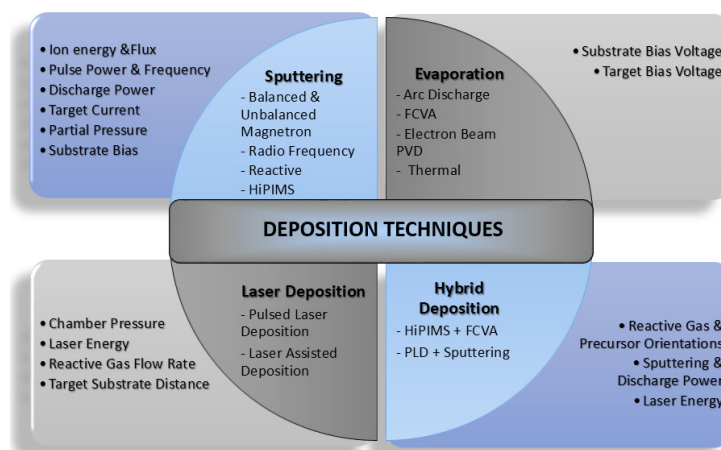


Figure 1. PVD methods to deposit hard coatings and the crucial process parameters for tuning the coating properties

Since commercialising the arc evaporation PVD technique in the early 1980s, researchers have made substantial technological advancements to enhance process efficiency and coating quality. Initial improvements focused on refining the quality and ionisation of coating materials [12]. These involved using higher-quality targets, employing high-purity reactive gases, and incorporating additional anode and plasma sources to boost the ionisation process [2,3] – subsequent enhancements centred on optimising deposition parameters. The key parameters significantly affecting defects include substrate bias, arc current, and reactive gas pressure. These studies indicated that optimising these factors is an auspicious, cost-effective, and practical approach to improving the stability and reliability of coatings suitable for large-scale industrial applications. Driven by technological advancements and increased market demand, the architecture of evaporated coatings has evolved into four distinct structures: mono, duplex, composite, functionally graded, and multilayer. These advancements have led to significant improvements in the tribological performance of coatings over time [13-15].

Numerous studies have shown that arc evaporation PVD multilayer architectures can be tailored to optimise the tribomechanical properties of coatings for complex technological applications [16-20]. Firstly, these multilayers prevent crack propagation at multiple-layer interfaces and across grain boundaries. Secondly, they combine the properties of each individual layer into a new structure with unique, enhanced characteristics. For example, one layer can have a low coefficient of friction, high hardness, and resistance to high-temperature oxidation, reducing friction and preventing cracks. In contrast, another layer provides high adhesion, plasticity, and elasticity, boosting the coating's mechanical strength. The simultaneous function of these layers gives the multilayer structure a distinctive range of properties, effectively preventing early failure of the coating. Additionally, the multilayer architecture significantly changes the wear mechanism due to transition zones between adjacent layers, which can hinder crack propagation and reduce stress. While this research area is advancing, there is an ongoing need to improve the structure and properties of these coatings. This drives the search for new protective coating compositions that can meet modern requirements, especially those that maintain the structural integrity of coated products under high mechanical stresses and temperatures, thereby extending their operational lifespan.

Despite the ongoing evolution of this research domain, there remains a continual need to improve the structure and properties of arc evaporated PVD multilayer coatings. A discernible trend has developed in the past decade towards increasingly complex compositions within the resultant coatings. The integration of novel metallic and gaseous components into vacuum arc coating, along with the addition of supplementary layers possessing unique physical and mechanical characteristics, necessitates the modernization of current equipment and the advancement of new programmable devices to expand the variety of coatings produced.

Functional Structure of the Device for Deposition of Arc Evaporated PVD Simple and Complex Composition Multilayer Coatings

Figure 2 illustrates the upgraded arc evaporated PVD system designed to synthesize multilayer coatings with simple and complex compositions. A feature of the update to the classic equipment is the addition of a two-channel control device, termed the “evaporator-injector” [21]. Channel 1 manages the operation of vacuum-arc evaporators, whereas Channel 2 governs the operation of gas starters. Consequently, operating two evaporators and two gas starters is feasible. The device comprises five blocks on separate boards: a device control unit, a relay switch circuit, a data input panel, a display panel, and a power supply. The central component of the device is a control unit built on a low-power 8-bit Atmel microcontroller. The relay switch circuit is designed to activate or deactivate each channel within a specified time frame. Setting the time parameters for the device's channels and selecting the mode and cycle of the control device's operation is accomplished manually via the control elements. Thus, the thickness of the vacuum-arc coating layers, along with the sequence of their application, can be regulated through the modes and duration of operation of the channels of the “evaporator-injector” control device.

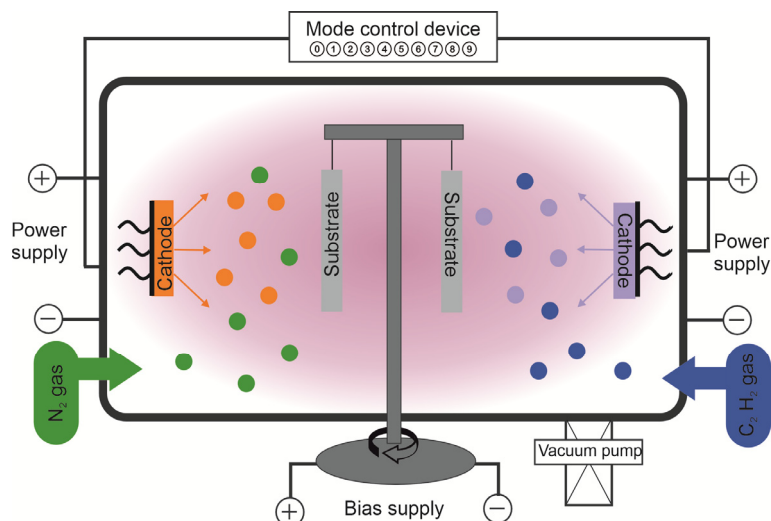


Figure 2. Schematic view of the arc evaporated PVD unit used to synthesize complex multilayer coatings

The “evaporator-injector” has 10 modes (modes 0–9). The time intervals for the operation of vacuum-arc evaporators and gas starters are set by parameters t_1 – t_4 . Here are details about the operating modes [21]:

1) Mode 0. Two vacuum-arc evaporators are activated alternately, while gas is continuously supplied to the vacuum chamber by one of the gas G injectors. The operating time of the evaporators is defined by time parameters t_1 for cathode 1 (metal 1 – Me_1) and t_2 for cathode 2 (metal 2 – Me_2). This operating mode permits the production of simple Me_1G/Me_2G -type multilayer coatings, such as TiN/ZrN or TiC/ZrC.

2) Mode 1. The first vacuum-arc evaporator operates continuously. The operating time of the second evaporator is determined by the time parameters: t_1 – the duration of the evaporator's off state, and t_2 – the duration of the evaporator's on state. Gas is continuously supplied to the vacuum chamber through one of the gas injectors. Consequently, the thickness of the Me_1G layer relies on the parameter t_1 , while the parameter t_2 governs the thickness of the Me_1Me_2G layer. This operating mode allows for the production of simple Me_1G/Me_1Me_2G type multilayer coatings, such as TiN/TiZrN or TiC/TiZrC.

3) Mode 2. Both channels (the vacuum-arc evaporator and gas injector control channels) operate synchronously. The operational duration of the evaporators and gas injectors is specified by the time parameters t_1 (cathode 1 – Me_1 , gas 1 – G_1) and t_2 (cathode 2 – Me_2 , gas 2 – G_2). This operating mode allows for producing simple Me_1G_1/Me_2G_2 -type multilayer coatings, such as TiN/ZrC or ZrN/TiC.

4) Mode 3. The first vacuum-arc evaporator (cathode 1 – Me_1) operates continuously, with gas (G_1) constantly supplied through the initial gas inlet. The operating time of the second evaporator (cathode 2 – Me_2) and the gas supply duration (G_2) through the second inlet are determined by time parameters: t_1 – duration of the off state of the vacuum-arc evaporator and inlet, t_2 – duration of the on state of the evaporator and inlet. Employing this operating mode enables the creation of simple multilayer coatings composed of compounds of the type $Me_1G_1/Me_1Me_2G_1G_2$, such as TiN/TiZrNC.

5) Mode 4. Channel 1 (cathode 1 – Me_1 and cathode 2 – Me_2) operates in mode 0, meaning the vacuum-arc evaporators are activated alternately. The duration of the evaporators is regulated by time parameters: t_1 – duration of the on state of the first evaporator, t_2 – duration of the on state of the second evaporator. Channel 2 (injector 1 – gas 1 (G_1) and injector 2 – gas 2 (G_2)) operates in mode 1, meaning gas 1 (G_1) is continuously supplied through the first gas inlet while gas 2 (G_2) is provided for the duration t_2 of the operation of the second evaporator (cathode 2 – Me_2). Using this operating mode facilitates the attainment of simple multilayer coatings composed of $Me_1G_1/Me_2G_1G_2$ type compounds, such as TiN/ZrCN.

6) Mode 5. Channel 1 (cathode 1 – Me_1 and cathode 2 – Me_2) operates in mode 1, i.e. the first vacuum arc evaporator (cathode 1 – Me_1) operates continuously, while the second vacuum arc evaporator (cathode 2 – Me_2) is activated for time t_2 . Channel 2 (injector 1 – gas 1 and injector 2 – gas 2) functions in mode 0, meaning the injectors are switched on alternately. The operational duration of each gas injector is defined by the time parameters: t_1 – the duration of the activated state of the first gas injector, and t_2 – the duration of the activated state of the second gas injector. This operating mode facilitates the production of $Me_1G_1/Me_1Me_2G_2$ -type multilayer coatings, such as TiC/TiZrN.

7) Mode 6. From this operating mode onwards, the device employs two timers: t_3 and t_4 . Both channels operate in mode 0. The duration of operation for each vacuum-arc evaporator and gas injector is governed by the following time parameters: t_1 – duration of the on-state of the first evaporator, t_2 – duration of the on-state of the second evaporator, t_3 – duration of the on-state of the first gas injector, t_4 – duration of the on-state of the second gas injector. The operational time parameters are selected as follows: $t_3 = t_1 + t_2$, $t_4 = n(t_1 + t_2) = nt_3$, where $n = 1$. Utilizing this operating mode allows for the production of complex multilayer coatings of $Me_1G_1/Me_2G_1/[Me_1G_2/Me_2G_2/Me_1G_2/Me_2G_2/...]$ -type, such as TiN/ZrN/[TiC/ZrC/TiC/ZrC/...].

8) Mode 7. Both channels operate synchronously. Channel 1 (cathode 1 – Me₁ and cathode 2 – Me₂) operates in mode 0, which means the vacuum-arc evaporators are activated alternately. The duration of the evaporators is determined by the time parameters: t₁ – the duration of the first evaporator's active state and t₂ – the duration of the second evaporator's active state. Channel 2 (injector 1 – gas 1 and injector 2 – gas 2) operates in mode 1, indicating that gas 1 is supplied continuously through the first gas injector, while the duration of the second gas injector is defined by the time parameters: t₃ – the duration of the second injector's inactive state and t₄ – the duration of the second injector's active state. Utilizing this operating mode permits the production of complex multilayer coatings from compounds of Me₁G₁/Me₂G₁/[Me₁G₁G₂/Me₂G₁G₂/Me₁G₁G₂/Me₂G₁G₂/...] -type, such as TiC/ZrC/[TiCN/ZrCN/TiCN/ZrCN/...].

9) Mode 8. Both channels operate synchronously. Channel 1 (cathode 1 – Me₁ and cathode 2 – Me₂) functions in mode 1, meaning the first vacuum-arc evaporator (cathode 1 – Me₁) operates continuously, while the operational duration of the second evaporator (cathode 2 – Me₂) is determined by the time parameters: t₁ – the duration of the second evaporator's inactive state and t₂ – the duration of its active state. Channel 2 (injector 1 – gas 1 and injector 2 – gas 2) operates in mode 0, indicating that the injectors are activated sequentially. The time parameters establish the operational duration of each gas starter: t₃ – the active state of the first injector and t₄ – the active state of the second injector. Employing this operating mode enables the acquisition of complex multilayer coatings of Me₁G₁/Me₁Me₂G₁/[Me₁G₂/Me₁Me₂G₂/Me₁G₂/Me₁Me₂G₂/...] -type, for example, TiC/TiZrC/[TiN/TiZrN/TiN/TiZrN/...].

10) Mode 9. Both channels operate synchronously in mode 1. Channel 1 (cathode 1 – Me₁ and cathode 2 – Me₂) functions in mode 1, meaning the first vacuum-arc evaporator operates continuously, while the operation duration of the second evaporator is determined by the time parameters: t₁ – duration of the off state of the second evaporator, and t₂ – duration of the on state of the second evaporator. Channel 2 (injector 1 – gas 1 and injector 2 – gas 2) also operates in mode 1, which indicates that gas 1 is supplied continuously through the first gas injector, with the operation duration of the second gas injector defined by the time parameters: t₃ – duration of the off state of the second injector, and t₄ – duration of the on state of the second injector. In this device's operating mode, various control algorithms can be implemented by setting the time parameters. Here are two of the most noticeable algorithms. The first one when t₁ = t₃ and t₂ = t₄. Employing this operational algorithm enables the production of multilayer coatings of Me₁G₁/Me₁Me₂G₁G₂-type, such as TiC/TiZrCN. The second one is when the time parameters of the device operation are chosen as follows: t₃ = t₁ + t₂, t₄ = n(t₁ + t₂) = nt₃. Utilising this operational algorithm enables the achievement of complex multilayer coatings from compounds of this type. Me₁G₁/Me₁Me₂G₁/[Me₁G₁G₂/Me₁Me₂G₁G₂/Me₁G₁G₂/Me₁Me₂G₁G₂/...], for instance, TiC/TiZrC/[TiCN/TiZrCN/TiCN/TiZrCN/...].

The initial results from operating the developed device in the laboratory for intensive ion-plasma technology research at the National Research Centre Kharkov Institute of Physics and Technology (KIPT) of the NAS of Ukraine confirmed its technical specifications.

EXPERIMENTAL PROCEDURE

Deposition

Using a two-channel control device enabled the fabrication of multilayer vacuum-arc WNbN/WNbC, WN/WC and NbN/NbC coatings. The coatings were obtained through the vacuum-arc evaporation of two tungsten (W) and niobium (Nb) cathodes, positioned on the same horizontal level at an angle of 90 degrees to one another in an upgraded Bulat-6 type installation. The cathodes were made by mechanical boring from ingots of the corresponding metals obtained by electron beam re-melting. The starting components of re-melting were pure tungsten (W content not less than 99.97 wt.%) and technical niobium (Nb content not less than 98.2 wt.%, main impurity Zr with the content between 1-1.4 wt.%).

Table 1. Technological parameters of coating deposition.

No.	Coating composition	I _d , A	I _f , A	U _b , V	Gas	P, Pa	T, h	Notes
1	2	3	4	5	6	7	8	9
1	WNbN/WNbC	130/120	0.5/0.5	200	N/C ₂ H ₂	0.4	1.0	VR: C ₂ H ₂ -10 s, N - 50 s
2	WNbN/WNbC	150/110	0.5/0.5	200	N/C ₂ H ₂	0.4	0.8	VR: C ₂ H ₂ - 5 s, N - 55 s
3	WNbN/WNbC	150/115	0.5/0.5	120	N/C ₂ H ₂	0.4	1.0	VR: C ₂ H ₂ - 5 c, N - 90 c
4	NbN/NbC	120	1.0	220	N/C ₂ H ₂	0.4	1.0	VR: C ₂ H ₂ -5 s, N - 55 s
5	WN/WC	170	1.0	220	N/C ₂ H ₂	0.4	1.0	VR: C ₂ H ₂ - 5 s, N - 55 s

Explanation of table columns:

1 – the number of the series of samples;

2 – the elemental composition of the coating;

3 – I_d, is the value of the cathodic arc current;

4 – I_f, is the value of the current of the focusing coils on the corresponding cathode;

5 – U_b, is the value of the negative bias voltage (potential) applied to the substrate;

6 – the composition of the reaction gas in the deposition chamber (nitrogen N or acetylene C₂H₂);

7 – P is the value of the reaction gas pressure in the deposition chamber;

8 – T is the duration of the coating deposition process (measured in hours);

9 – the notes explaining the sample rotation characteristics and exposure time near the appropriate evaporator or with the proper reaction gas in the chamber, seconds: CR – constant rotation, VR – variable rotation.

The stainless-steel plates of 12X18H9T (corrosion-resistant high-temperature steel, analogue to AISI321 (USA)) were used as substrates. The size of each sample was 15 mm × 15 mm × 2.5 mm. The surface of the substrates before coating deposition was prepared in several stages. The first stage involved mechanical grinding and polishing, executed with abrasive materials of varying grain sizes on a paper or fabric base, while employing forced cooling with water on a manual grinding and polishing device. The second stage consisted of mechanical fine polishing using diamond pastes with diamond particle dispersion ranging from 6 μm to 0.1 μm. After the mechanical processing to remove any grease and impurities, the samples were washed in isopropyl alcohol. The third sample preparation stage was plasma-electrolytic polishing in an electrolyte from an aqueous solution (3 wt.%) of ammonium sulfate (NH₄)₂SO₄. Such polishing clearly leads to a loss of sample mass, but the amount of such loss does not exceed 0.2 mg/cm². In the end, the last stage of preparing the substrate surface – ion bombarding – was applied. The vacuum chamber was evacuated to a pressure of 0.001 Pa. Then a negative bias potential of 1000 V was applied to the substrate holder, which cleaned and activated the surface of the substrates by bombarding it with metal ions emitted from the evaporator cathode. The duration of bombarding was around 5 minutes. After the cleaning operation was completed, the bias voltage was reduced to the value necessary to deposit the coating of the selected type and composition.

The vacuum chamber of the arc installation has cylindrical form, with an internal diameter of 600 mm and a height of 800 mm. This, a vacuum chamber volume is approximately 0.22 m³. As demonstrated in the experiment, the installation's pumping system efficiently reduced the working gas pressure from 0.4 Pa to a residual vacuum value of 1·10⁻³ Pa within 1 second, ensuring a swift and reliable process. The accuracy of setting the internal channel switching time of the developed two-channel control device is 1 second. The interval between deactivating one of the gas injectors and activating the other is approximately 1 second. This duration is sufficient to reduce the pressure in the vacuum chamber to the ultimate residual value of 0.001 Pa. Given these parameters, the proximity of both gases in the chamber during the coating process is unlikely. When producing a multilayer coating, the pumping speed of the chamber was monitored by observing the current pressure value using a vacuum gauge. For the formation of the carbide layer WNbC, WC, and NbC, the acetylene (C₂H₂) was introduced into the vacuum chamber and dissociated during the coating process. We maintained a strict control over the pressure of reaction gases in the vacuum chamber, ensuring stability and quality in the process.

Equipment and Procedure of Microstructure Analysis

The morphology and cross-sections of multilayer vacuum-arc WNbN/WNbC, WN/WC and NbN/NbC coatings were examined using the JEOL JSM 7600F high-resolution field emission scanning electron microscope (FE-SEM, JEOL Ltd., Tokyo, Japan) in secondary electron (SE) imaging mode. The microscope operated within an accelerating voltage range of 20-30 kV, with a magnification capability of up to 100,000 times. The maximum resolution of the raster microscope reached 2.5 nm at an accelerating voltage of 30 kV.

To obtain precise results from the SEM technique, we adhered to the author's methodology for specimen preparation. Specifically, the coatings' cross-section was prepared using a mechanical polishing method. Specimens measuring approximately 20 mm in length and 4 mm in width were cut from bulk samples employing a diamond wire-cutting machine. These specimens were then embedded in phenolic resin and ground down to #1200 using silicon carbide (SiC) abrasive grit paper. Subsequently, they were polished with diamond suspensions featuring particle sizes of 1, 3, and 6 microns, and finally rinsed with distilled water before being dried with warm air. This methodology enabled us to create mirror-like cross-sectional specimens and capture high-quality images of the coatings and the substrate. Figure 3 presents images illustrating the SEM's specimen preparation process.

The ImageJ software was utilized for the SEM image analysis. In summary, the obtained images were transferred into ImageJ and analyzed using two distinct techniques: the first employed 8 bits (designated as 8B) and the second referred to as "R G B" (Red, Green, Blue colors). These techniques were utilized to detail the features of typical structural defects (macroparticles, pores, inclusions, etc.) including their locations, quantities, and areas (maximum, minimum, and mean).

RESULTS AND DISCUSSION

Figure 3 illustrates the typical view of the surface and cross-section of multilayer vacuum-arc WNbN/WNbC coatings. Evidence of the intercolumnar fracture of the upper layer can be seen in the coating's surface. The coating exhibits a well-defined layered structure with dense growth. Light grey layers are attributed to the WNbN, whereas dark grey layers correspond to the WNbC. The subtle zigzag shape of the layers results from applying negative substrate bias during deposition, causing ion bombardment on the WNbN/WNbC layers while the added atoms advance to the substrate surface [22]. In work [23] observed that sputtered layers exhibit a cupola-like microstructure at a working pressure of 0.67 Pa without substrate bias. In contrast, work [24] reported a wave-like layer structure arising from the kinetic energy of the incident ionic species influenced by the rf-bias, which enhances the velocity and surface mobility of the ad-atoms, consequently impacting the crystalline structure. The cross-section image allows for measuring the coating's total thickness, which is 568.7 nm.

The impact of hydrogen, which emerges during the dissociation process, on the properties of vacuum-arc coatings is presently insufficiently studied due to the specificities inherent in the technology utilized for their production. Historically, nitrogen was used as the reaction gas to create vacuum-arc coatings. Exploring alternative gases – namely

oxygen and acetylene – is in its early stages. A thorough analysis of the characteristics exhibited by the produced coatings leads to the conclusion that the potential impact of hydrogen on their properties, as observed in our experiments, is relatively minimal. This conclusion is supported by the observation that the coating displays a qualitatively dense structure in cross-section.

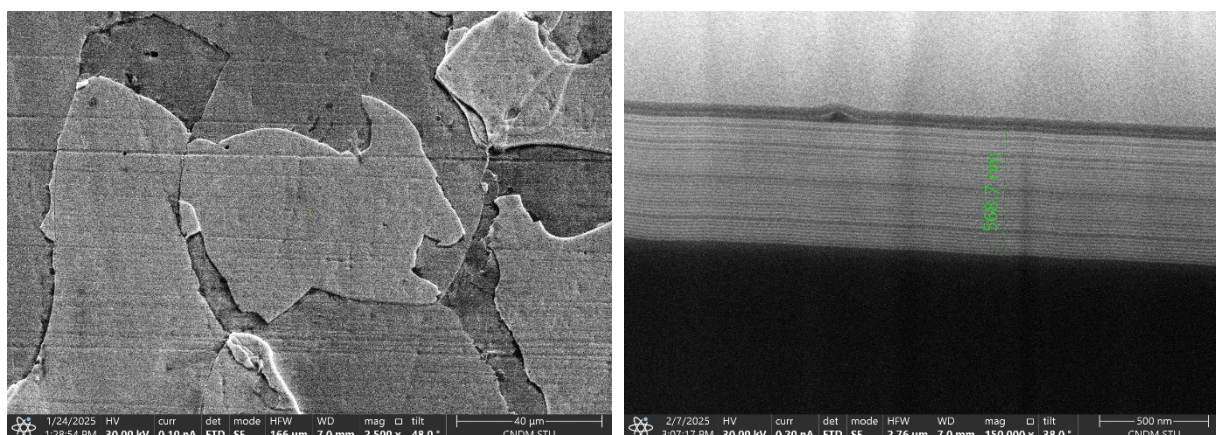


Figure 3. SEM images of the surface and cross-sections of multilayer vacuum-arc WNbN/WNbC coatings and the total coating thickness

CONCLUSIONS

To enhance the chances of synthesis of both simple and complex multilayer vacuum-arc coatings within one technological deposition cycle of arc evaporation PVD technology, a two-channel control device – “evaporator-injector” – was created to control the functions of vacuum-arc evaporators and the gas introduction ports in the vacuum chamber of the Bulat-6 installation.

This device enabled the production of multilayer vacuum-arc coatings such as WNbN/WNbC, WN/WC, and NbN/NbC, all of which feature nanometer thickness and excellent structural integrity.

Acknowledgments

This project has received funding through the EURIZON project, which is funded by the European Union under grant agreement No.871072. Additional funding was received from the EU NextGenerationEU through the Recovery and Resilience Plan for Slovakia under the project No. 09I03-03-V01-00028.

ORCID

- © O.V. Maksakova, <https://orcid.org/0000-0002-0646-6704>; © V.M. Beresnev, <https://orcid.org/0000-0002-4623-3243>
 © S.V. Lytovchenko, <https://orcid.org/0000-0002-3292-5468>; © D.V. Horokh, <https://orcid.org/0000-0002-6222-4574>
 © B.O. Mazilin, <https://orcid.org/0000-0003-1576-0590>; © I.O. Afanasieva, <https://orcid.org/0000-0002-9523-9780>
 © M. Čaplovičová, <https://orcid.org/0000-0003-4767-8823>; © M. Sahul, <https://orcid.org/0000-0001-9472-500X>
 © V.A. Stolbovoy, <https://orcid.org/0000-0001-7734-0642>

REFERENCES

- [1] D.M. Mattox, *Handbook of Physical Vapor Deposition (PVD) Processing*; (Elsevier Science & Technology Books: Amsterdam, The Netherlands, 2007).
- [2] A. Baptista, F.J.G. Silva, J. Porteiro, J.L. Míguez, and G. Pinto, “Sputtering Physical Vapour Deposition (PVD) Coatings: A Critical Review on Process Improvement and Market Trend Demands,” *Coatings*, **8**, 402 (2018). <https://doi.org/10.3390/coatings8110402>
- [3] Y. Deng, W. Chen, B. Li, C. Wang, T. Kuang, and Y. Li, “Physical vapor deposition technology for coated cutting tools: A review,” *Ceram. Int.* **46**, 18373–18390 (2020). <https://doi.org/10.1016/j.ceramint.2020.04.168>
- [4] A. Pak, M. Masoudi, and H. Elmkhah, “Effect of ultrasonic peening on the surface properties of nano-layered CrN/CrAlN coating deposited by CAPVD method on D3 tool steel,” *Surf. Interfaces*, **28**, 101618 (2021). <https://doi.org/10.1016/j.surfint.2021.101618>
- [5] K.S. Lim, Y.S. Kim, S.H. Hong, G. Song, and K.B. Kim, “Influence of N₂ Gas Flow Ratio and Working Pressure on Amorphous Mo–Si–N Coating during Magnetron Sputtering,” *Coatings*, **10**, 34 (2020). <https://doi.org/10.3390/coatings10010034>
- [6] M.R. Alhafian, J.B. Chemin, Y. Fleming, L. Bourgeois, M. Penoy, R. Useldinger, F. Soldera, *et al.*, “Comparison on the Structural, Mechanical and Tribological Properties of TiAlN Coatings Deposited by HiPIMS and Cathodic Arc Evaporation,” *Surf. Coat. Technol.* **423**, 127529 (2021). <https://doi.org/10.1016/j.surfcoat.2021.127529>
- [7] B.C.N.M. de Castilho, A.M. Rodrigues, P.R.T. Avila, R.C. Apolinario, T. de Souza Nossa, M. Walczak, *et al.*, “Hybrid Magnetron Sputtering of Ceramic Superlattices for Application in a next Generation of Combustion Engines,” *Sci. Rep.* **12**, 2342 (2022). <https://doi.org/10.1038/s41598-022-06131-9>
- [8] A. Jacob, *Effect of Micro-blasting on Characteristics and Machining Performance of PVD AlTiN Coated Cutting Tools; Master of Technology*; (National Institute of Technology: Rourkela, India, 2015).
- [9] J.Y. Sheikh-Ahmad, and T. Morita, “Tool coatings for wood machining: Problems and prospects,” *For. Prod. J.* **52**, 43–51 (2002).

- [10] S. Grundas, *Advances in Induction and Microwave Heating of Mineral and Organic Materials*, (IntechOpen, Rijeka, Croatia, 2011).
- [11] K. Holmberg, and A. Mathews, *Coatings Tribology—Properties, Mechanisms, Techniques and Application in Surface Engineering*, 2nd ed. (Elsevier: Amsterdam, The Netherlands, 2009).
- [12] I.I. Aksenov, A.A. Andreev, V.A. Belous, V.E. Strelnitsky, and V.M. Khoroshikh, *Vacuum Arc: Plasma Sources, Coating Deposition, Surface Modification*, (Naukova Dumka, Kyiv, 2012).
- [13] X. Li, et al., “Cathodic arc evaporation for hard and decorative coatings: A review.” *Surface Engineering*, **34**(8), 553-570 (2018). <https://doi.org/10.1080/02670844.2017.1397537>
- [14] J.C. Sánchez-López, et al., “A review on superhard nanocomposite coatings: Recent progress and future directions.” *Materials Science and Engineering: R: Reports*, **91**, 1-46 (2015). <https://doi.org/10.1016/j.mser.2015.02.001>
- [15] D. Depla, et al., “Comparison of reactive magnetron sputtering and cathodic arc deposition for the synthesis of TiN and TiAlN thin films.” *Thin Solid Films*, **519**(15), 5047-5054 (2011). <https://doi.org/10.1016/j.tsf.2010.12.122>
- [16] B.K. Rakhadilov, O.V. Maksakova, D.B. Buitkenov, M.K. Kylyshkanov, A.D. Pogrebnyak, V.P. Antypenko, Ye.V. Konoplianchenko, “Structural-phase and tribo-corrosion properties of composite Ti₃SiC₂/TiC MAX-phase coatings: an experimental approach to strengthening by thermal annealing”, *Appl. Phys. A*, **128**, 145 (2022). <https://doi.org/10.1007/s00339-022-05277-7>
- [17] M. Beresnev, S.V. Lytovchenko, O.V. Maksakova, A.D. Pogrebnyak, V.A. Stolbovoy, S.A. Klymenko, and L.G. Khomenko, “Microstructure and high-hardness effect in WN-based coatings modified with TiN and (TiSi)N nanolayers before and after heat treatment: experimental investigation,” *High Temperature Material Processes*, **25**(4), 61–72 (2021). <https://doi.org/10.1615/HighTempMatProc.2021041565>
- [18] O.V. Maksakova, S. Zhanyssov, S.V. Plotnikov, P. Konarski, P. Budzynski, A.D. Pogrebnyak, V.M. Beresnev, et al., “Microstructure and tribomechanical properties of multilayer TiZrN/TiSiN composite coatings with nanoscale architecture by cathodic-arc evaporation,” *J. Mater. Sci.* **56**, 5067–5081 (2021). <https://doi.org/10.1007/s10853-020-05606-2>
- [19] C. Ducros, and F. Sanchette, “Multilayered and nanolayered hard nitride thin films deposited by cathodic arc evaporation. Part 2: Mechanical properties and cutting performances,” *Surface and Coatings Technology*, **201**(3-4), 1045-1052 (2006). <https://doi.org/10.1016/j.surfcoat.2006.01.029>
- [20] Y.X. Ou, J. Lin, S. Tong, W.D. Sproul, and M.K. Lei, “Structure, adhesion and corrosion behavior of CrN/TiN superlattice coatings deposited by the combined deep oscillation magnetron sputtering and pulsed dc magnetron sputtering,” *Surf. Coat. Technol.* **293**, 21–27 (2016). <https://doi.org/10.1016/j.surfcoat.2015.10.009>
- [21] I.V. Serdiuk, V.O. Stolbovyi, A.V. Dolomanov, and V.M. Domnich, “Modernization of Vacuum-Arc Deposition Technology of Multilayer Nanostructured Coatings,” *Metallofiz. Noveishie Tekhnol.* **44**(4), 547–563 (2022). (in Ukrainian). <https://doi.org/10.15407/mfint.44.04.0547>
- [22] J. Xu, T. He, L. Chai, L. Qiao, P. Wang, and W. Liu, “Growth and characteristics of self-assembled MoS₂/Mo-S-C nanoperiod multilayers for enhanced tribological performance,” *Sci. Rep.* **6**, 25378 (2016). <https://doi.org/10.1038/srep25378>
- [23] K. Järrendahl, I. Ivanov, J.-E. Sundgren, G. Radnóczy, Z. Czigany, and J.E. Greene, “Microstructure evolution in amorphous Ge/Si multilayers grown by magnetron sputter deposition,” *J. Mater. Res.* **12**, 1806–1815 (1997). <https://doi.org/10.1557/JMR.1997.0249>
- [24] C. Cancellieri, E. Klyatskina, M. Chiodi, J. Janczak-Rusch, and L.P.H. Jeurgens, “The Effect of interfacial Ge and RF-bias on the microstructure and stress evolution upon annealing of Ag/AlN multilayers,” *Appl. Sci.* **8**, 2403 (2018). <https://doi.org/10.3390/app8122403>

БАГАТОШАРОВІ ПОКРИТТЯ WNbN/WNbC, WN/WC ТА NbN/NbC:

СТРАТЕГІЯ ВАКУУМНО-ДУГОВОГО ОСАДЖЕННЯ ТА ОЦІНКА МІКРОСТРУКТУРИ

О.В. Максакова^{a,b}, В.М. Береснев^b, С.В. Литовченко^b, Д.В. Горох^b, Б.О. Мазілін^b, І.О. Афанасьєва^{b,d},
М. Чапловичова^c, Мартин Сахул^a, В.А. Столбовой^d

^aІнститут матеріалознавства, Словацький технологічний університет у Братиславі,
вул. Яна Ботту 25, 917 24, Трнава, Словаччина

^bХарківський національний університет імені В.Н. Каразіна, пл. Свободи, 4, 61000 Харків, Україна

^cЦентр нанодіагностики матеріалів, Словацький технологічний університет у Братиславі,
Вазова 5, 812 43, Братислава, Словаччина

^dНаціональний науковий центр «Харківський фізико-технічний інститут», 61108, вул. Академічна 1, м. Харків, Україна

Реактивні гази, такі як азот, кисень і гази на основі вуглецю (наприклад, ацетилен), додають до згенерованого плазмового потоку для створення покриттів з хімічних сполук, включаючи нітриди, оксиди і карбіди. Керуванням швидкості додавання газу можна контролювати стехіометричний склад покриття, який впливає на його кристалічну структуру і спектр властивостей. З огляду на це для осадження багат шарових карбідних/нітридних покриттів на основі W і Nb у динамічно мінливій атмосфері газів азоту та ацетилену було використано метод вакуумно-дугового осадження (PVD). Для керування роботою вакуумно-дугових випарників і портів введення газів у вакуумній камері установки використовувався двоканальний пристрій керування «випарник-інжектор». Матеріалом підкладок для осадження покриттів була корозійностійка жароміцна сталь марки 12X18H9T. Катоди W (99,97 мас. %) і Nb (98,2 мас. %) виготовляли механічним розточуванням зливків з відповідних металів, отриманих електронно-променевим переплавом. У роботі описано стратегію осадження вакуумно-дугових багат шарових покриттів WNbN/WNbC, WN/WC і NbN/NbC з нанометровою товщиною шарів і проведено попередню оцінку їхньої мікроструктури. Представлені багат шарові системи ще не вивчені і становлять значний науковий інтерес з точки зору процесу синтезу та експериментального дослідження властивостей.

Ключові слова: керамічні покриття; нітрид вольфраму; карбід вольфраму; нітрид ніобію; карбід ніобію; вакуумно-дугова обробка; мікроструктура